Crack initiation and propagation analysis at welds – assessing the total fatigue life of complex structures

Rissinitiierung und Wahrscheinlichkeitsanalyse an Schweißverbindungen – Abschätzung der Lebensdauer von komplexen Strukturen

J. Baumgartner[1], R. Waterkotte[2]

The fatigue strength of complex welded structures may differ highly from that of a simple test specimen. The reason for this observation is in most cases the high amount of crack propagation on the total fatigue life. The aim of this work is to describe the complex failure mechanism with a two-phase model. In this model, the crack initiation and crack propagation phase are assessed separately. The fatigue life until initiation of a crack is derived by notch stresses, calculated using stress averaging or the critical distance approach. The macro crack propagation is determined by fracture mechanics. The methods, which are available to determine the fatigue life until crack initiation, lead to reliable results. The determination of stress intensity factors proved to be demanding. Variations were observed depending on the calculation approach used. For application in industry, the applied approaches should be improved further.

Keywords: Weld start and stop position / crack initiation / crack propagation

Das Schwingfestigkeitsverhalten von komplexen Bauteilen unterscheidet sich in vielen Fällen stark von dem einfacher Proben. Diese meist im Abgleich zwischen Berechnung und experimenteller Prüfung gemachte Beobachtung kann häufig über den hohen Anteil des Rissfortschritts an der Gesamtlebensdauer erklärt werden. Ziel dieses Beitrags ist es, das komplexe Schwingfestigkeitsverhalten über ein zwei-Phasen Modell zu beschreiben, in dem die Anriss- und die Rissfortschrittsphase separat betrachtet werden. Die Anrissschwingspielzahl wird hierbei über den Spannungsmittelungs- und Spannungsabstandsansatz berechnet, die anschließende Rissfortschrittsphase über bruchmechanische Methoden. In einer Gegenüberstellung von experimentell ermittelter und berechneter Lebensdauer zeigte sich eine gute Übereinstimmung für das Versagenskriterium technischer Anriss. Bei der bruchmechanischen Bewertung erwies sich die Berechnung der Spannungsintensitätsfaktoren als nicht trivial. Für die industrielle Anwendbarkeit empfiehlt sich daher eine Erweiterung und Optimierung der zur Verfügung stehenden numerischen Werkzeuge.

Schlüsselwörter: Schweißnahtanfang und -ende / Risseinleitung / Rissfortschritt

[1] Fraunhofer-Institute for Structural Durability and System Reliability (LBF), Darmstadt, Germany
[2] Schaeffler Technologies GmbH & Co. KG, Herzogenaurach, Germany

Corresponding author: J. Baumgartner, Fraunhofer-Institute for Structural Durability and System Reliability (LBF), Darmstadt, Germany,
E-Mail: joerg.baumgartner@lbf.fraunhofer.de

1 Introduction

In the development phase of components and assemblies, a multitude of requirements have to be met. Along with consistent continuation of lightweight design, development times should be further shortened and in addition production costs should be kept as low as possible. While a high degree of experience and engineering are required for an innovative component design, the strength of the components must first be consecutively determined numerically and later experimentally.

Great advances have been made in the last few years, especially in the fatigue strength assessment of welded connections that form potential weak spots in components. With the local stress approach [1, 2] or the stress averaging approach according to Neuber [3, 4] that has been "rediscovered" in the last years, a quick and reliable fatigue strength analysis can be obtained using software tools.

Despite these advances, there are still some details for which a reliable fatigue strength assessment is not possible. To be mentioned here are, among others, weld start and stop positions as can be found, for example, on welded shifting components of a gear unit, *Fig. 1*.

High stress concentrations appear at weld start and stop positions and a high degree of conservativeness is achieved when assessing these stress concentrations with the local stress approach. The possible reasons for this are manifold. Due to the very high stress concentrations, elastic as well as plastic support effects increasingly appear (size effects, macroscopic-yielding). In addition, the crack propagation phase frequently takes up a large portion of the total fatigue life. Both effects lead to an underestimation of the fatigue strength for the start and stop positions. These effects are observed in a fatigue strength assessment of the shifting components, *Fig. 2*. A comparison between numerically calculated (with the notch stress approach using a reference radius of $r = 0.05$ mm) and experimental fatigue strength shows a difference of a factor of 5 in the direction of load above the calculated SN-curve.

For this paper, the task thus consists in systematically extending the assessment method for start and stop positions, taking into account the particular notch shapes at weld ends and the technical state of the art. This is achieved by considering fatigue tests under constant amplitude loading of several specimens, in which the crack initiation and propagation phase is recorded. Evaluation of the results is done classically according to the local stress approach using a reference radius, with local stresses determined according to Neuber and methods of fracture mechanics with the aid of finite element analyses. The duration of crack propagation is determined on the basis of numerically and analytically ascertained results, applying fracture-mechanical characteristics from the literature and experiments.

2 Fatigue assessment concept

Various concepts are available for assessing the fatigue strength of weld seams [5]. In the automobile industry and that of its suppliers, mostly stress-based concepts are used since they are easy to apply and they allow a calculation of the fatigue life via unit load cases. The nominal stress approach, structural

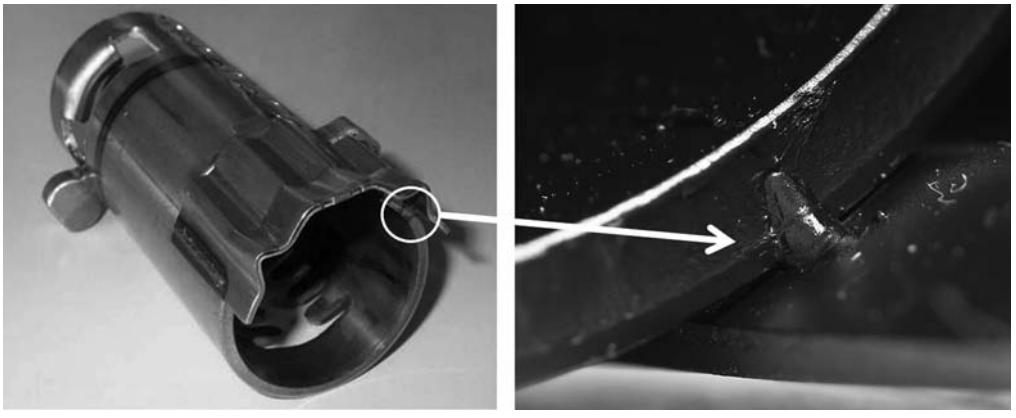

Figure 1. Shifting component
Bild 1. Schaltkomponente

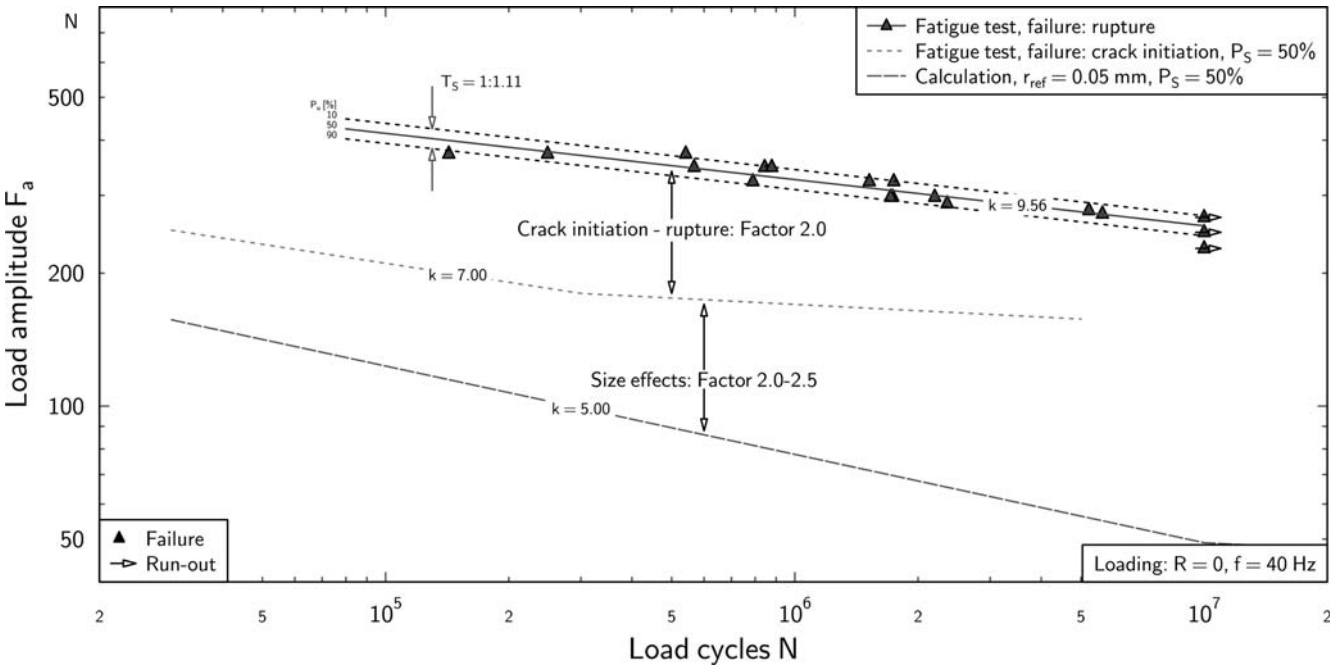

Figure 2. Comparison between numerically derived and experimentally determined S–N curves
Bild 2. Vergleich zwischen berechneter und experimentell ermittelter Bauteilwöhlerlinie

hot spot stress approach and local stress approach are among them, *Fig. 3*. But in special cases fracture mechanics is also used for calculative fatigue life analysis.

In this work, the emphasis was on design with local stress approaches and with fracture-mechanical methods. These two methods are briefly described in what follows.

2.1 Local stress approaches

Notches in a component cause local concentration of stress that decisively influence the fatigue strength of a component. In the case of welded connections, they are mostly welt toe notches or weld root notches at which cracks can initiate under cyclic load, *Fig. 4*.

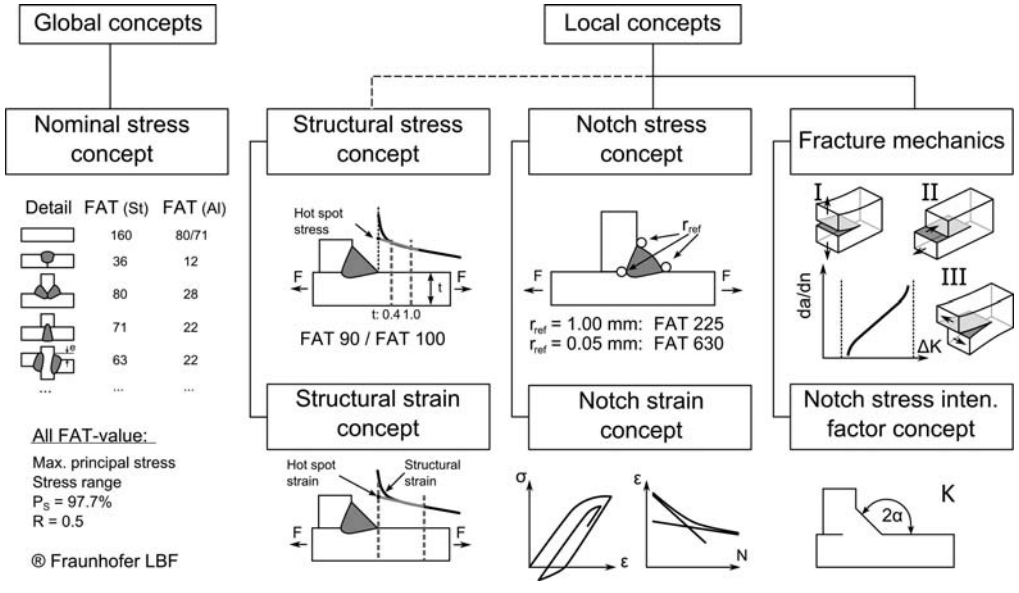

Figure 3. Fatigue assessment concepts for welded joints
Bild 3. Konzeptauswahl zur schwingfesten Bewertung von Schweißverbindungen

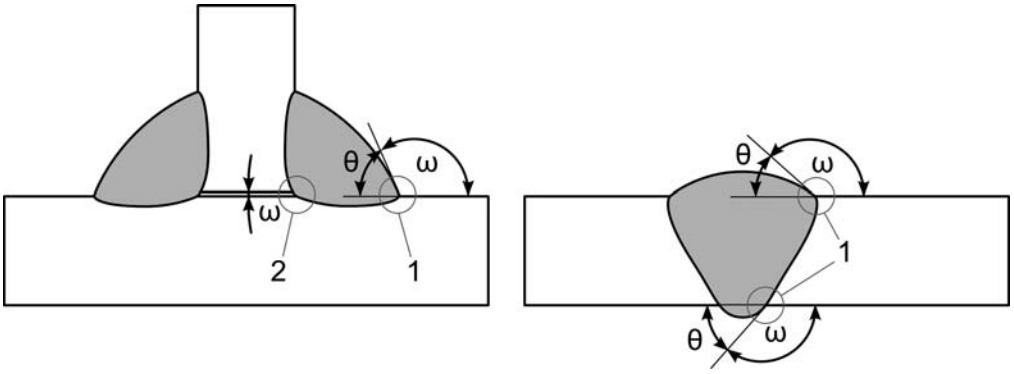

Figure 4. Notches of a weld seam: 1) weld toe/transition notch and 2) weld root notch
Bild 4. Kerben an Schweißnähten: 1) Nahtübergangskerbe und 2) Nahtwurzelkerbe

A numerical assessment of these notches with the local stress approach is done via fictitious rounding with a reference radius. The fictive notch radius r_f = 1 mm was derived for welded joints connecting thick plates, based on the micro support according to Neuber in a "worst case" consideration (the real radius approaches zero and the notch opening angle is $\omega = 0°$) [6]. Due to the fictive enlargement of the real radius, the "support effects" appearing in the sharp notches can be taken into account in a fatigue strength analysis.

An application of the local stress approach with the radius r_f = 1.0 mm for thin sheet connections with sheet thicknesses t < 5.0 mm is in most cases not possible, since either the cross section would be too severely weakened or the stress flow in the welded connection would be too severely altered. For an assessment of root notches at welded thin sheet connections, a reference radius of r_{ref} = 0.05 mm was thus first introduced and successfully applied in industrial use at spot-welded and later also at laser-welded thin sheet connections [2, 7, 8], where the failure originates in the weld root. The choice of the radius r_{ref} = 0.05 is arbitrary. Every small enough notch radius would yield similar results, since the calculated local stresses can be interpreted as a fracture-mechanical magnitude [1]. Therefore no support effects are considered with this approach.

2.2 Stress averaging approach according to Neuber

In the application of the reference radius r_{ref} = 0.05 mm to seam transition notches, larger differences appear in the tolerable stress between the transition notch and the weld root [9]. The difference can be explained by support effects that are covered in the case of the concept with r_f = 1.0 mm, but not when using smaller radii. Such support effects can be separately taken into account, for example, with the aid of Neuber's stress averaging approach in an assessment of weld seam notches at thin sheet connections [4, 10].

By means of stress averaging, a modified stress σ_{avg} can be calculated that takes into account the stress curve in an area of the notch ligament to be determined that is perpendicular to the direction of the seam, *Fig. 5*.

$$\sigma_{avg} = \frac{1}{\rho^*} \int_0^{\rho^*} \sigma(x)\, dx \qquad (1)$$

This can be done, for example, on the basis of the stress $\sigma(x)$ calculated with the aid of the Finite-Element method. The averaging length, also called microstructure length ρ^*, is in this context regarded as a material parameter.

2.3 Theory of critical distances (TCD)

Another method is the theory of critical distance (TCD). The original idea for deriving the critical distance from fracture-mechanical considerations is from [11]. A unitary theoretical model has been developed since 1997 [12–15]. The concept builds on the stress averaging approach according to Neuber [6] and the critical distance approach according to Peterson [16]. In addition, the connection to the approach of el Haddad et al. which describes the threshold behaviour for the growth of short cracks, was established by the material characteristic length parameter, called "critical distance", which Taylor

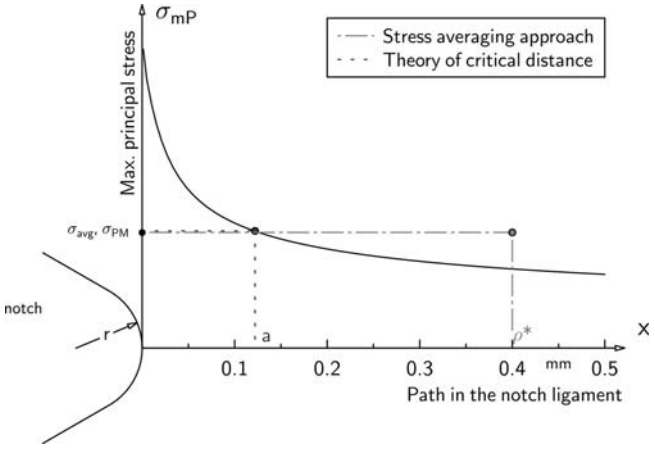

Figure 5. Calculation of an effective notch stress applying the stress averaging approach proposed by Neuber as well as the critical distance approach

Bild 5. Berechnung versagensrelevanter Spannungen mit dem Spannungsmittelungs- und Spannungsabstandsansatz

designates as L [17]. The theory of critical distance (TCD) assumes a relationship between the so called endurance limit of the material and the threshold of the stress intensity factor. The only parameter is the critical distance L.

$$L = \frac{1}{\pi} \cdot \left(\frac{\Delta K_{th}}{\Delta \sigma_D} \right)^2 \tag{2}$$

The theory of critical distance differs into the point method (PM), line method (LM), surface method (AM) and volume method (VM). With the point method, the position of the evaluation location is chosen at a distance a = L/2 in the notch ligament. If in a notched component the stress at this location reaches the fatigue limit of an un-notched specimen, the fatigue limit of the component should be reached, too.

$$\Delta \sigma_{PM,D} = \Delta \sigma \left(\frac{L}{2} \right) = \Delta \sigma(a) = \Delta \sigma_D \tag{3}$$

With the line method, an averaged stress is determined over a segment of 2 · L. This corresponds to the stress averaging approach according to Neuber (2 · L = ρ*). As for the point method, the endurance limit is reached, if the averaged stress over the distance 2 · L reaches the endurance limit of an unnotched specimen. Since the surface and volume methods are not used in this work, they are not described.

2.4 Weld start and stop positions

Even though weld start and stop positions (also referred to as weld terminations) commonly occur in welded structures, there exist quite few recommendations in literature how the fatigue strength at these positions should be assessed. For the nominal stress approach, only two FAT classes including termination points (No. 324 and No. 612) are considered in the IIW-Recommendations [18]. Inside the IIW-Recommendations as well as in further rules and guidelines, no specific recommendations are given for the application of the structural or notch stress approach related to start and stop positions.

Only few publications explicitly consider weld terminations or, more in general, stress gradients in weld seam direction within the notch stress approach [19–23]. The main challenge is on one hand the modelling of the weld at the termination points, especially the transition between weld toe and weld root notch. On the other hand higher endurable notch stresses have been calculated in comparison to seam welds without start and stop positions. These finding have been connected to two effects: the statistical size effects (the length or the area of the highly stresses region) and support effects due to different stress gradients. In some of these publications the crack propagation phase is already considered in the assessment.

2.5 Fracture-mechanical methods

Assuming a crack capable of growing with length a_0, the residual fatigue life of a component can be estimated with fracture-mechanical methods. If the crack is sufficiently deep, linear-elastic fracture-mechanics (LEFM) can be applied.

In linear-elastic fracture-mechanics, the stress intensity factor K represents the amount of the stress stress singularity at the crack tip. For a fatigue assessment its range ΔK is used. In this connection, a difference has to be according to the type of stress. In mode I, the crack is opened by normal stress, in modes II and III, shearing stresses operate in different slip directions.

$$\Delta K = K_{max} - K_{min} = \Delta \sigma \cdot \sqrt{\pi a} \cdot Y \tag{4}$$

With a cyclic load, the crack growth per load cycle is described by the crack propagation rate da/dN, which can be experimentally determined with the

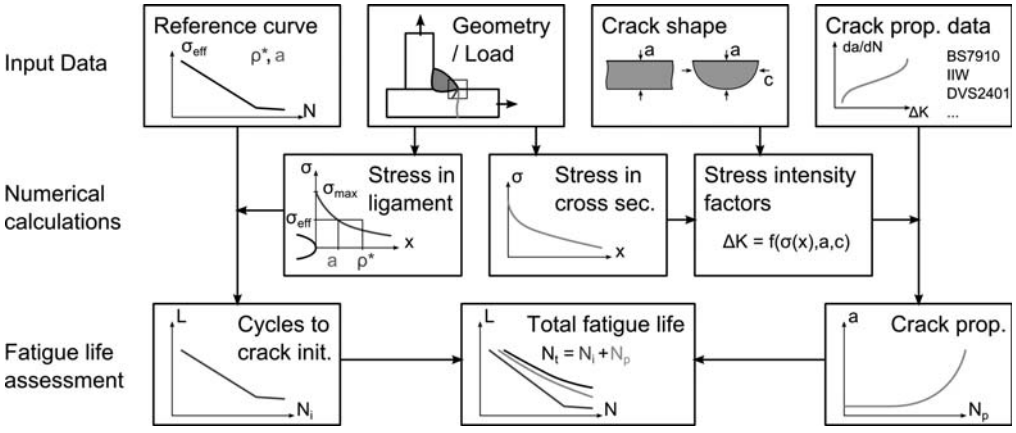

Figure 6. Assessment approach for the estimation of the fatigue life
Bild 6. Bewertungsansatz zur Ermittlung der Gesamtlebensdauer

aid of test samples. With the experimentally determined fracture-mechanical characteristics C and m and a numerical or analytical determination of the ΔK-a curve, a crack propagation life for the component can be determined with the Paris law [24].

$$\frac{da}{dN} = C \times \Delta K^m \tag{5}$$

The parameters C and m are dependent on the material; the factor C is additionally influenced by the stress ratio R. The R ratio can be taken into account by using the crack propagation approach of Forman/Mettu [25].

2.6 Application to complex welded structures

The fatigue assessment of weld start and stop positions is done on the basis of a two-phase model in which the calculation of the crack initiation life and the crack propagation life are separately done, *Fig. 6*.

The crack initiation life N_i is calculated with the local stress approach, with stress averaging according to Neuber using a microstructure length of $\rho^* = 0.4$ mm and a reference radius $r_{ref} = 0.05$ mm.

For the crack propagation life N_p, stress intensity factors are first determined depending on the depth of the crack (ΔK-a curve). The "extended finite element method" (XFEM) with the ABAQUS program, the ADAPCRACK3D program from the University of Paderborn and weight functions were applied [26]. In the second step, the crack propagation life is calculated with the aid of the Paris equation [24]. Fracture-mechanical characteristics from the British Standard and experimentally determined values are used for this [27].

Validation of the design method is done in direct comparison with the fatigue strength tests.

3 Experimental investigations

Fatigue strength tests were carried out on welded structures, a shifting component, a welded flat specimen with a sharp root notch and a longitudinal stiffener, *Fig. 7*. All fatigue tests have been performed using constant amplitudes. In the case of the shifting component (sheet thickness t = 1 mm) and the flat specimen (t = 3 mm), the area of crack initiation was at the end of a laser beam weld seam. In the case of

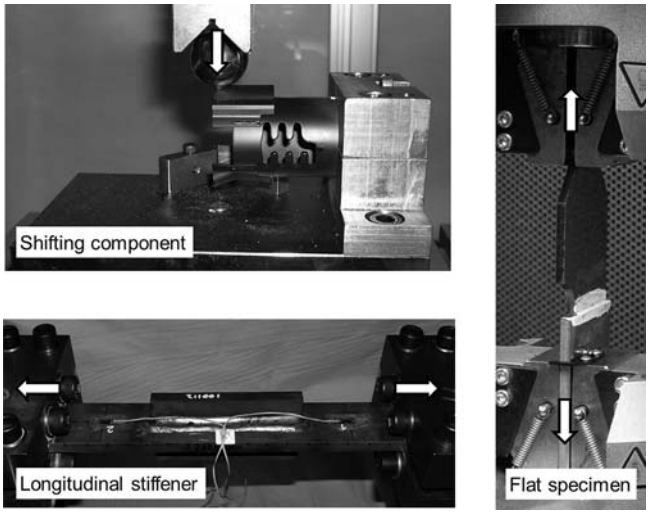

Figure 7. Specimens considered for the fatigue evaluation
Bild 7. Den Untersuchungen zugrunde liegende Probekörper

the longitudinal stiffener (t = 12 mm), the crack emanated from the end of the stiffener, a short but highly stressed weld seam section. The angle of seam incline was on average θ = 60°.

The tests were performed with a stress ratio of R = 0. In the case of the longitudinal stiffener, a mean load independence was identified in the fatigue tests, which results from tensile residual stress induced by the welding process [28]. Therefore, tests with R = –1 were included in the evaluation additionally.

Optical procedures were used for crack identification in the tests described here. In the case of the longitudinal stiffeners, crack identification was done with the aid of a zinc oxide paste that changes colour with crack initiation. For this, the critical seam weld area was monitored with a digital camera during the test and following the test an assessment of the crack propagation was carried out. Two cracks of depths a = 0.1 mm and a = 0.5 mm were detected.

In the case of the shifting component and the flat specimen, the cracks initiated at hidden weld root notch. Thus in the case of these components, crack detection was done via thermo-elastic stress analysis (TSA) [29]. The crack depth ascertained with this process is a ≈ 0.1 mm.

3.1 Fatigue assessment

Finite element models for calculation of the local weld seam stresses were prepared for all samples. Global geometry based on the nominal dimensions was used for this; the weld seam geometry was mapped on the basis of micrographs and 3-D scans. For the longitudinal stiffener, transition radii were measured in the range of r = 0.02 mm to r = 0.55 mm. The median was r ≈ 0.05 mm. For the shifting component and the flat specimen, measurement of the transition notches is more difficult, since sharp weld toot notches are present. These notches were rounded out with a radius of r = 0.05 mm [1].

An experimental strain analysis was carried out on all components and the models or boundary conditions were adapted in such a way that a good conformity between calculated and measured strains was obtained.

3.2 Crack initiation

An assessment of the crack initiation life was done with the local stress approach, the stress averaging approach and the critical distance approach. For this, the stress course in the notch ligament, from which the required stresses, the maximum notch stress σ_e, the notch stress σ_{avg} averaged according to Neuber

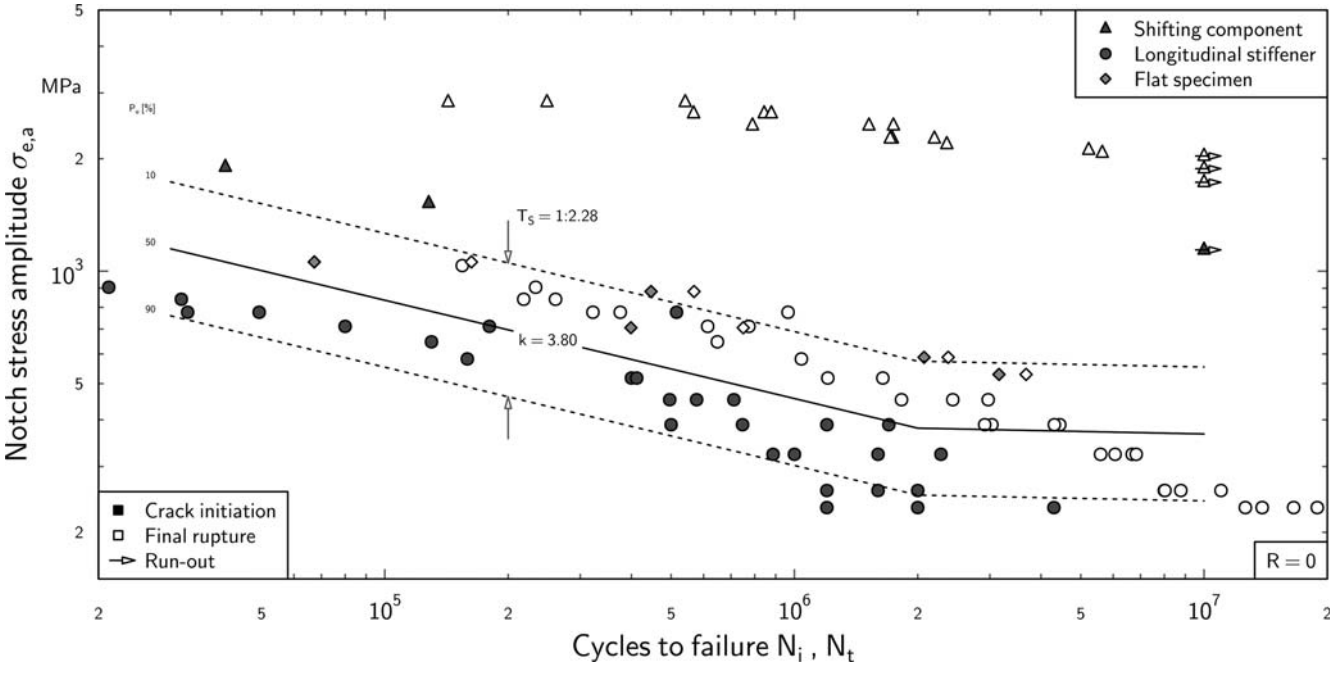

Figure 8. Comparison of test results based on maximum notch stresses (r = 0.05 mm)
Bild 8. Vergleich der ertragbaren maximalen Kerbspannungen (r = 0,05 mm)

and the stress σ_{PM} at a distance a* can be derived, was taken from the calculation models.

In the case of an assessment with the notch stress approach, the endurable local stresses have a very high scatter of $T_s = 1 : 2.40$, *Fig. 8*. The test results at the longitudinal stiffeners show the least endurable stresses. The shifting component and the butt weld where cracks emerge at the seam ends show higher capacities.

In the evaluation of components with local stresses averaged according to Neuber for a microstructure length of $\rho^* = 0.4$ mm, there is a clear reduction in the scatter to $T_s = 1 : 1.70$ for the crack initiation lives [10], *Fig. 9*.

The differences result primarily from the different slopes (flatter slope of the SN-curve for the flat specimen in comparison to that of the longitudinal stiffener) and the load cycle numbers at the knee point. They are at $N_k = 1 \cdot 10^5$ for the shifting component and $N_k > 2 \cdot 10^6$ for the longitudinal stiffeners.

For application of the critical distance approach, the material-characteristic length parameter according to Taylor for the flat specimen and the shifting component were determined with the aid of the experimental investigations. Since the crack starts in the weld seam in the case of the flat specimen and the shifting component, the material data were identified for this material condition. A fracture-mechanical threshold of $\Delta K_{th} = 300\ \mathrm{Nmm^{-3/2}}$ was determined in tests and a so-called endurance limit of the weld metal ($\sigma_{a,D} = 418$ MPa) was estimated on basis of the materials hardness. With these data, a critical distance of $a^* = 0.023$ mm results for the point method (PM) and $\rho^* = 0.09$ mm for the line method (LM).

For the flat specimen and shifting component, the local effective stress based on the point method delivers good conformity with the material SN-curve of the weld seam for the "incipient crack" failure criterion, *Fig. 10*.

For the material of the longitudinal stiffeners, ΔK_{th} was not determined. For this reason, the tests cannot be taken up in the comparison.

3.3 Fracture mechanics

Material characteristics are required for calculating the macro-propagation of the crack. They can be experimentally determined on CT specimens, for example. Since these characteristics are not subject to overly large variation (in comparison to the fatigue strength of un-notched material samples), there is in addition still the possibility of using statistical average values or values from material data collections, e.g., the British Standard 7910.

Along with the fatigue tests on welded structures, crack propagation curves for the material of the shifting component and the flat specimen were thus

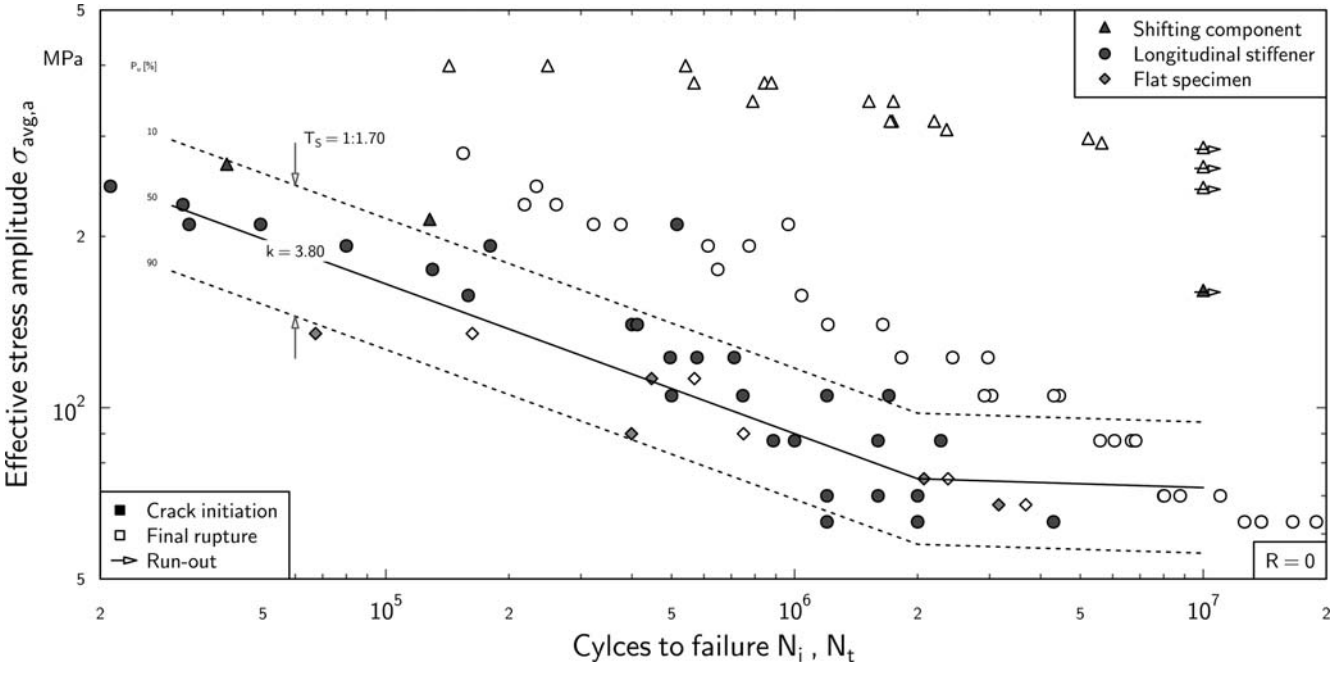

Figure 9. Comparison of test results based on notch stresses derived by averaging according to Neuber
Bild 9. Vergleich der ertragbaren Spannungen auf Basis des Spannungsmittelungsansatzes nach Neuber

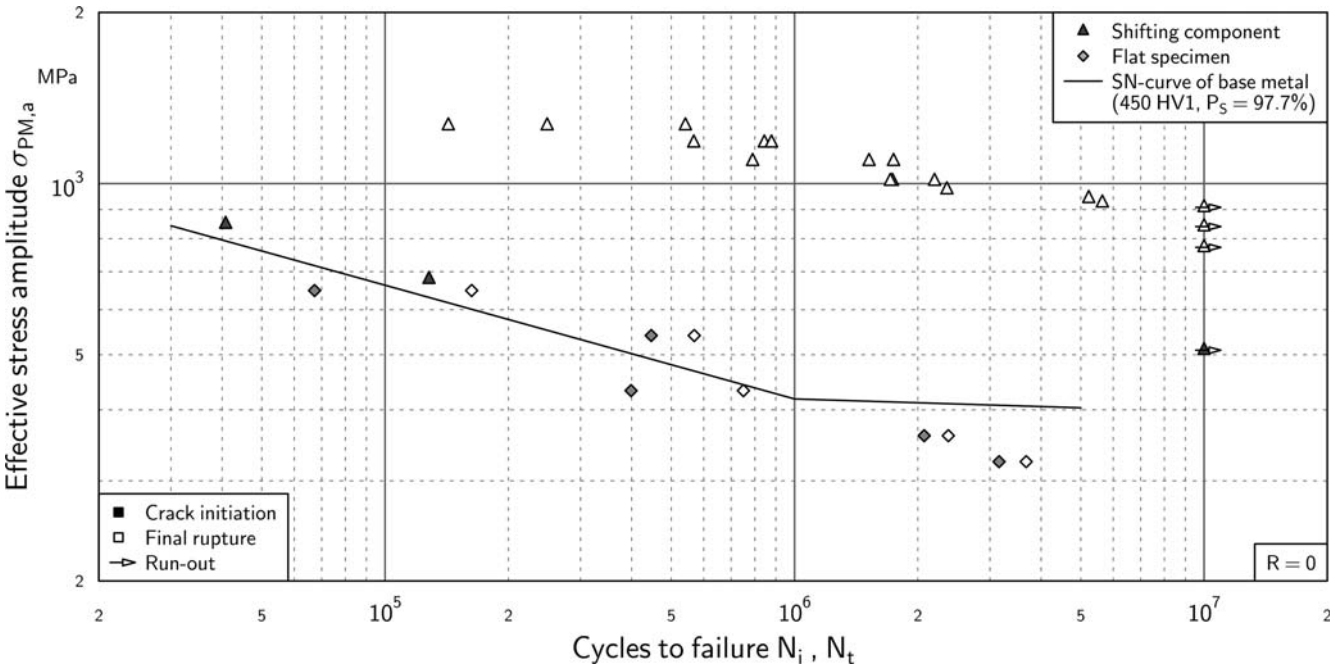

Figure 10. Results for crack initiation (filled symbols) using modified notch TCD Point-Method and SN-curve of the weld seam material

Bild 10. Ertragbare Spannungen für das Versagenskriterium Anriss auf Basis des Spannungsabstandansatzes im Vergleich zur Festigkeit des Grundwerkstoffs

determined on CT specimen. In the tests there was no significant difference between the characteristic curves for the base material and the weld metal, *Fig. 11*. Thus only the averaged curve is shown. The difference from the characteristic curves in the British Standard is slight.

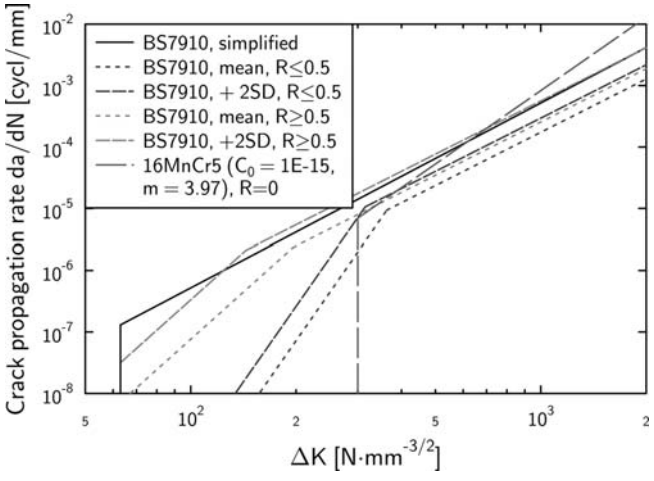

Figure 11. Crack propagation rates according to BS7910 and experimentally determined results for the material 16MnCr5

Bild 11. Experimentell ermittelte Rissfortschrittskurven für den Werkstoff 16MnCr5 im Vergleich zu BS7910

3.3.1 Longitudinal stiffeners

At the longitudinal stiffeners, the crack first runs through the heat-affected zone and then through the base material. Since no characteristic values have been determined for the different areas, crack propagation rates for the base metal S460 from literature were used [30].

For the crack propagation calculation at the longitudinal stiffener, weight functions according to Glinka were used. With them it is possible, to analytically describe the change in the stress intensity factor depending on the depth of the crack. For this, along with the initial dimension of the crack (a/2c = 0.1 mm/13.0 mm), the stress course in the failure-relevant cross section is used as an input value. These stresses were derived from Finite-Element models. An integration of the stresses in the middle of the specimen (Section A-A) leads to a nominal stress σ_n^*, which is 20% higher than the nominal stress σ_n in the base plate, *Fig. 12*.

Calculation of the crack propagation SN-curve was done via integration of the crack propagation equation. Welding residual stresses have been estimated from a weld process simulation and considered as mean stresses [31].

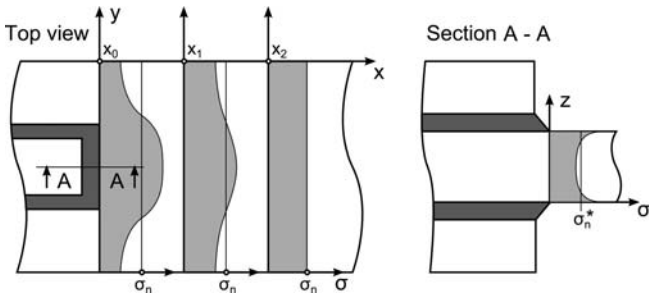

Figure 12. Stress distribution at the longitudinal stiffer close to the weld

Bild 12. Spannungsverteilung an dem Ende der Längssteifen

The development of the crack shape during the fatigue loading was identified in the fatigue test by a block program and compared to the analytical solution, *Fig. 13*. It can be seen, that without any modifications the anaytically derived crack growth phase is only 1/3 of the experimental one. The main reason for this effect is the fast growth in width; the ratio of the crack width and crack depth does not match. If the a/c-ratio is not taken from the crack growth calculation, but adepted to the experimental values, the crack growth phase is nearly doubled. Futhermore, if a correction of the nominal stresses is included in a way that during crack propagation σ_n^* is gradually lowered to σ_n an even better correlation can be identified [28].

In addition, stress intensity factors were determined with XFEM calculations in ABAQUS [32]. Simplifying, a plain and elliptical crack at a distance of 0.01 mm from the seam transition notch was used due to numerical reasons, *Fig. 14*. By this approach the change of the stress intensity factors with increasing crack dimensions could be derived numerically. Since the welding residual stresses have not been transferred to the XFEM-model, crack propagation curves for the load ratio R = 0.5 have been used.

By using the two modifications a fair agreement between analytically and experimentally derived crack propagation phase can be identified, *Fig. 15*. The use of the XFEM leads to nearly the same crack propagation life as the analytical solutions.

3.3.2 Flat specimen

The stress intensity factors required for calculation of the crack propagation were determined for the flat specimen with the aid of the XFEM, by the weight function approach and using the software AdapCrack3D.

For the XFEM analysis, the weld end was established as the location of crack initiation. Since the direction of the crack's growth is unknown in advance of the tests, and also could not be unequivocally determined on the basis of the tests, it was established by engineering considerations. The crack propagation analysis was carried out in a simplified fashion on the basis of weight functions. It was calculated for two crack initiation points: Starting from a highly stressed welded end and from the centre of the seam weld. Additionally, the crack propagation was determined by the software AdapCrack3D.

The comparison of calculated and experimentally determined crack propagation shows a difference of more than one magnitude in the direction of the load cycle, *Fig. 16*.

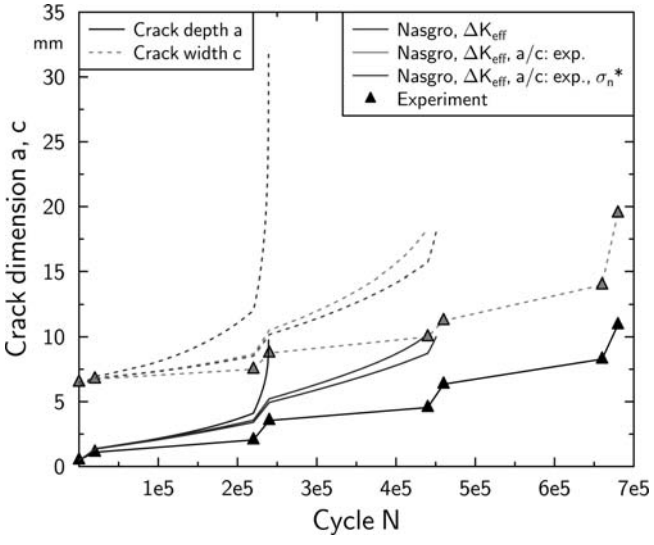

Figure 13. Comparison between calculated and experimental crack growth at the longitudinal stiffener

Bild 13. Vergleich zwischen berechnetem und experimentell ermitteltem Rissfortschritt an den Längssteifen

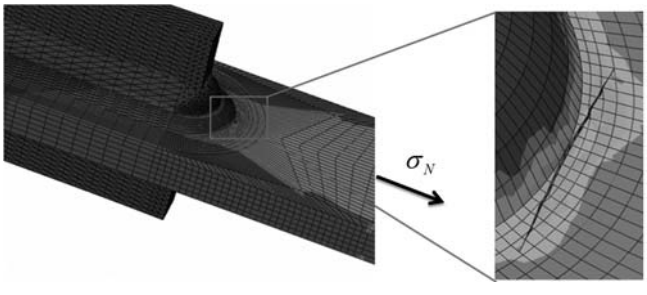

Figure 14. Determination of stress intensity factors depending on the crack length by XFEM

Bild 14. Ermittlung der Spannungsintensitätsfaktoren in Abhängigkeit der Risstiefe mittels XFEM

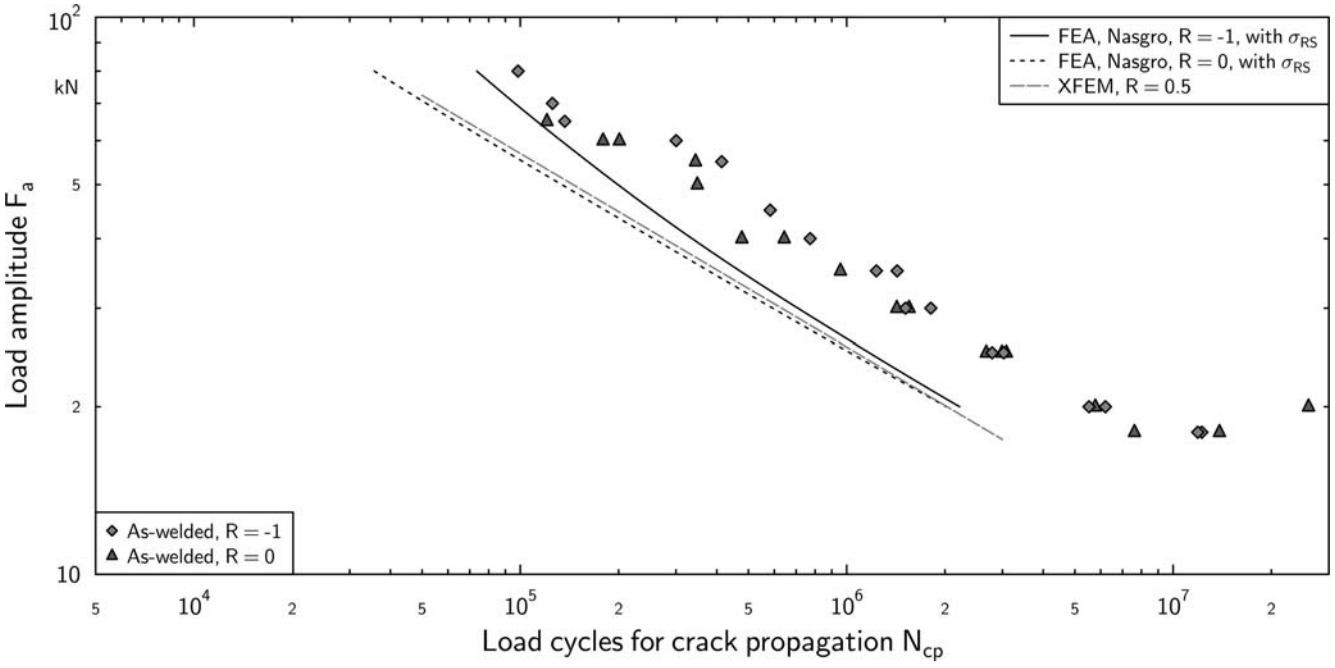

Figure 15. Longitudinal stiffener: Numerically and experimentally determined S–N curves for crack propagation
Bild 15. Vergleich zwischen berechneter und experimentell ermittelter Rissfortschrittslebensdauer an den Längssteifen

4 Assessment of the results

The investigation for assessing the fatigue strength of weld seam ends, using the example of a shifting component, presents the advantages and disadvantages that can appear with application of the assessment approaches based on local stresses and methods of fracture mechanics and shows how they can be used in practice.

For an analysis of the crack initiation life, the local stress approach using maximum notch stresses with r = 0.05 mm leads to a high scatter of T_s =

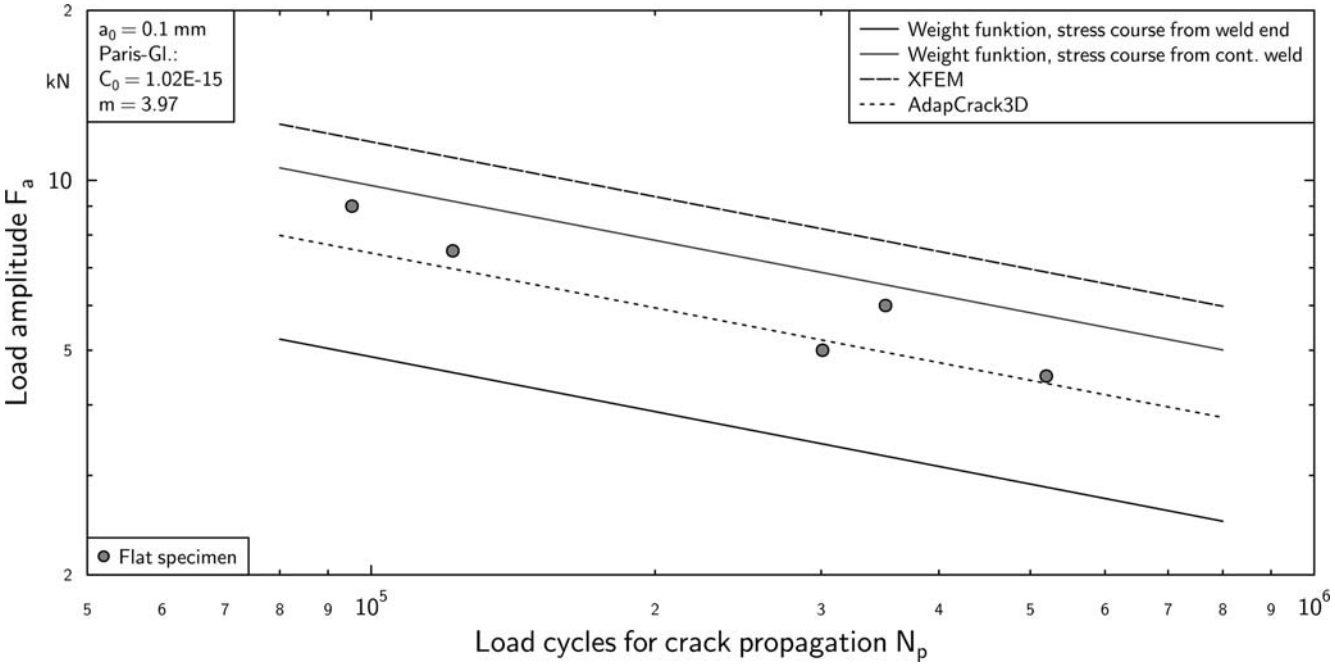

Figure 16. Flat specimen: Numerically and experimentally determined SN-curves for crack propagation
Bild 16. Vergleich zwischen berechneter und experimentell ermittelter Rissfortschrittslebensdauer an den Flachproben

1 : 2.28. This high scatter can be explained by support effects, which are not covered with this radius. In contrast to the notch stress approach, the stress averaging approach according to Neuber proves to be a more reliable method. The longer local fatigue life of sharp weld notches and weld ends can be assessed reliable by this approach.

In contrast to the crack initiation assessment, a reliable crack propagation analysis proves to be far more difficult.

For the longitudinal stiffeners, a conservative assessment was obtained. Two main reasons can be accounted for this result:

- An integration of the stress course in the cross section of the weld, which are used for an analytical crack propagation analysis, shows a 20% higher nominal stress. For small crack length, the fast crack growth can be reproduced. But with increasing crack propagation, the plate at both sides of the specimen builds a "support" for the crack front and leads consecutively to a reduction in the crack growth rate. An analytical crack propagation analysis cannot map these changes in the load path.
- The maximum stresses at weld ends are quite high, but so are the stress gradients, both, in depth and width direction. For an analytical analysis, the stress gradients in depth direction are used. But the stress gradients at the surface are not considered. For the longitudinal stiffener, this effect leads to a much faster crack growth rate and a shorter fatigue life.

Both reasons show the limitation of the analytical methods: Since only a one-dimensional stress course is used, effects of load (re-)distribution with increasing crack dimensions and stress gradients normal to the stress course lead in most cases to a quite conservative fatigue assessment.

The XFEM-method also leads to quite conservative results. The reasons behind this result are different: The crack propagation rates for a high load ratio had to be used since the welding residual stresses could not be imported in the program. Additionally, a plane crack was assumed, but in reality the crack shape is three-dimensional.

For the flat specimens the same reasons are valid. In addition, a multiple crack initiation in the load carrying weld seam might have occurred. Cracks might have started from the weld end and from the continuous weld. This would lead to a decrease in the overall fatigue crack growth phase.

Since the cracks did start from a hidden weld root notch, the real behaviour could not be identified exactly.

For the shifting component, which has a substantially more complex structure compared to the other components, no calculation of crack propagation was carried out. One reason was the large differences in the stress intensity factors observed already in the case of the "simple" flat specimens and longitudinal stiffeners. Another reason is a contact between two components, due to which the stress intensity factor is reduced significantly.

5 Summary and outlook

In the investigations it turned out that, depending on geometry, the type of load and sheet thickness, the crack propagation can exhibit a decisive portion of the total fatigue life. This applies in particular to the shifting component considered, for which a tolerable strength that was lower by a factor of five was determined with the local stress approach in comparison to the test.

With the assessment of the fatigue strength, the stress averaging approach according to Neuber proved to be suitable for calculating (linear-elastic) failure-relevant local stresses with which an analysis of the lifetime up to the crack initiation can be reliably carried out. This was also shown for the assessment according to the theory of critical distance with the point method, as described by Taylor.

Various approaches were followed for the crack propagation analysis. The linear–elastic fracture mechanics is an easily applicable method for the assessment of the crack growth in welded components, if analytical solutions can be applied. However, it has its drawbacks if the problem is no longer two-, but three-dimensional. There exist few approaches, which can include the stress gradients in both directions. In these cases, the application of Finite–Element calculations may be useful or even necessary. The analytical approaches finally reach their limits, if the influence of stress redistribution due to changes of the load path in a complex structure has to be covered.

For industrial use, the available numerical methods should be further improved so as to reliably ob-

tain the desired estimation quality in various applications. This would allow the lightweight design potential of welded structures to be used to a greater extent.

6 References

[1] G. Zhang, M. Eibl, S. Singh, O. Hahn, J. Kurzok, *Welding Cutting*, *1*, 96, **2002**.

[2] M. Eibl, C. M. Sonsino, H. Kaufmann, G. Zhang, *Int. J. Fatigue*, *25*, 719, **2003**.

[3] H. Neuber, Kerbspannungslehre, 2 ed., Springer Verlag, **1958**.

[4] G. Zhang, C. M. Sonsino, R. Sundermeier, *Int. J. Fatigue*, *37*, 24, **2012**.

[5] D. Radaj, C. M. Sonsino, W. Fricke, Fatigue assessment of welded joints by local approaches, Woodhead Publishing Limited, **2006**.

[6] H. Neuber, *Konstruktion*, *20*, 245, **1968**.

[7] G. Zhang, B. Richter, *Fatigue Fract. Eng. Mater. Struct.*, *23*, 499, **2000**.

[8] F. de Bruyne, A. Hoppe, VDI Tagung 2006: Berechnung und Simulation im Fahrzeugbau, **2006**.

[9] K. Störzel, J. Baumgartner, T. Bruder, H. Hanselka, *Materials Testing*, *53*, 418, **2011**.

[10] J. Baumgartner, E. Ince, H. Schmidt, (in review), *Weld. World*, **2015**.

[11] K. Tanaka, *Int. J. Fract.*, *22*, 39, **1983**.

[12] P. Lazzarin, R. Tovo, G. Meneghetti, *Int. J. Fatigue*, *19*, 647, **1997**.

[13] D. Taylor, The theory of critical distance: A new perspective in fracture mechanics, London: Elsevier BV, **2007**.

[14] L. Susmel, *Fatigue Fract. Eng. Mater. Struct.*, *27*, 391, **2004**.

[15] D. Bellett, D. Taylor, S. Marco, E. A. G. J. Mazzeo, T. Pircher, *Int. J. Fatigue*, *27*, 207, **2005**.

[16] R. Peterson, Stress concentration factors, John Wiley & Sons, **1974**.

[17] M. el Haddad, T. Topper, K. Smith, *Eng. Fract. Mech.*, *11*, 573, **1979**.

[18] A. Hobbacher, Ed., Recommendations for fatigue design of welded joints and components, Welding Research Council, Bulletin 520, **2009**.

[19] M. Kaffenberger, M. Vormwald, *Materialwiss. Werkstofftech.*, *42*, 874, **2011**.

[20] M. Malikoutsakis, G. Savaidis, *Fatigue Fract Engng Mater Struct*, *37*, 782, **2014**.

[21] J. Baumgartner, T. Bruder, H. Hanselka, *Int. J. Fatigue*, *33*, 65, **2012**.

[22] M. Kaffenberger, M. Malikoutsakis, G. Savaidis, M. Vormwald, *Computational Material Science* **2012**, *52*, 287.

[23] C. Fischer, W. Fricke, *International Institute of Welding*, XIII-2543-14, **2014**.

[24] P. Paris, F. Erdogan, *J. Basic. Eng*. **1963**, *85*, 528.

[25] H. A. Richard, M. Sander, Ermüdungsrisse, Wiesbaden: Vieweg+Teubner, GWV Fachverlage GmbH, **2009**.

[26] R. Goyal, G. Glinka, *Weld. World* **2013**, *57*, 625.

[27] British Standard BS 7910:2005, Guide on methods for assessing the acceptability of flaws in metallic structures, **2005**.

[28] J. Baumgartner, PhD-Thesis, Technical University Darmstadt, Fraunhofer Verlag, Stuttgart, **2014**.

[29] N. Harwood, W. Cummings, Thermoelastic Stress Analysis, Bristol, Philadelphia, New York: Adam Hilger, **1991**.

[30] M. Vormwald, *Materials Testing* **2011**, *53*, 98.

[31] I. Varfolomeev, S. Moroz, M. Brand, D. Siegele, J. Baumgartner, IWM Bericht W 17/2011, **2011**.

[32] R. Waterkotte, J. Baumgartner, Q. Ai, *Materials Testing* **2013**, *55*, 529.

Received in final form: January 23th 2015 T 367

